Preprint
UCRL-JC-137408

Dislocation Dynamics using Anisotropic Elasticity: Methodology and Analysis

M. Rhee, J.S. Stolken, V.V. Bulatov, T. Diaz de la Rubia, H.M. Zbib, J.P. Hirth

This article was submitted to Dislocation 2000, Gaithersburg, MD, June 19-22, 2000

U.S. Department of Energy
Lawrence Livermore National Laboratory

June 15, 2000

Approved for public release; further dissemination unlimited

DISCLAIMER

This document was prepared as an account of work sponsored by an agency of the United States Government. Neither the United States Government nor the University of California nor any of their employees, makes any warranty, express or implied, or assumes any legal liability or responsibility for the accuracy, completeness, or usefulness of any information, apparatus, product, or process disclosed, or represents that its use would not infringe privately owned rights. Reference herein to any specific commercial product, process, or service by trade name, trademark, manufacturer, or otherwise, does not necessarily constitute or imply its endorsement, recommendation, or favoring by the United States Government or the University of California. The views and opinions of authors expressed herein do not necessarily state or reflect those of the United States Government or the University of California, and shall not be used for advertising or product endorsement purposes.

This is a preprint of a paper intended for publication in a journal or proceedings. Since changes may be made before publication, this preprint is made available with the understanding that it will not be cited or reproduced without the permission of the author.

This report has been reproduced directly from the best available copy.

Available electronically at http://www.doe.gov/bridge

Available for a processing fee to U.S. Department of Energy
and its contractors in paper from
U.S. Department of Energy
Office of Scientific and Technical Information
P.O. Box 62
Oak Ridge, TN 37831-0062
Telephone: (865) 576-8401
Facsimile: (865) 576-5728
E-mail: reports@adonis.osti.gov

Available for the sale to the public from
U.S. Department of Commerce
National Technical Information Service
5285 Port Royal Road
Springfield, VA 22161
Telephone: (800) 553-6847
Facsimile: (703) 605-6900
E-mail: orders@ntis.fedworld.gov
Online ordering: http://www.ntis.gov/ordering.htm

OR

Lawrence Livermore National Laboratory
Technical Information Department's Digital Library
http://www.llnl.gov/tid/Library.html

Dislocation Dynamics using Anisotropic Elasticity: Methodology and Analysis

Moon Rhee, James S. Stolken, Vasily V. Bulatov and Tomas Diaz de la Rubia
Lawrence Livermore National Laboratory, Livermore, CA 94550

and

Hussein M. Zbib and John P. Hirth (Emeritus)
Washington State University, Pullman, WA 99164

Abstract

A numerical methodology to incorporate anisotropic elasticity into three-dimensional dislocation dynamics codes has been developed, employing theorems derived by Lothe (1967), Brown (1967), Indenbom and Orlov (1968), and Asaro and Barnett (1976). The formalism is based on the stress field solution for a straight dislocation segment of arbitrary orientation in 3-dimensional space. The general solution is given in a complicated closed integral form. To reduce the computation complexity, look-up tables are used to avoid heavy computations for the evaluation of the angular stress factor ($\sum_{ij}$) and its first derivative term ($\sum'_{ij}$). The computation methodology and error analysis are discussed in comparison with known closed form solutions for isotropic elasticity. For the case of Mo single crystals, it is shown that the difference between anisotropic and isotropic elastic stress fields can be as high as 15% close to the dislocation line, and decreases significantly far away from it. This suggests that short-range interactions should be evaluated based on anisotropic elasticity, while long-range interaction can be approximated using isotropic elasticity.

1. Introduction

Brown [1] developed a two-dimensional theorem to evaluate the stress field of an arbitrary dislocation configuration, where the field point and the dislocation line are co-planar. The stress field of a general dislocation in three-dimension was first developed by Indenbom and Orlov [2]. An alternative derivation with simpler expressions was given by Asaro and Barnett [3] where the resultant stress field for a given dislocation segment is expressed in terms of the so called angular stress factor and its derivative term for an infinite straight dislocation.

3D dislocation dynamics models to date employ isotropic elasticity theory to investigate the bulk behavior of single crystal composed of many dislocations. For some materials, using isotropic theory may not be appropriate. For example, in Cu the anisotropic effect is strong and leads to the formation of stacking fault tetrahedron. The objective of this paper is to provide a generalized approach to incorporate anisotropic elasticity into dislocation dynamics codes. Asaro and Hirth [4] investigated the equilibrium configuration of a three-fold node of dislocations in bcc α iron using full anisotropic elasticity theory and later extended by Stolken [5] to study different types of possible junction reactions in bcc metals. Recently, Raabe [6] applied anisotropic elasticity for numerical simulations of 3D dislocation statics where the stress fields for finite small angle tilt boundaries were investigated by direct evaluations of the integral equations]. Shenoey *et al.* [7] employed anisotropic elasticity for their dynamic simulation to study the behavior of partial junction dislocations in an fcc metal. However, direct calculation of stress fields using anisotropic elasticity becomes computationally heavy since the closed integrals, in general, need to be evaluated

numerically. In this paper, we provide a methodology for the purpose of reducing the computational effort for problems that may require a large number of dislocation segments by the use of memory, or look-up tables.

2 Background

The stress field of an infinitely long straight dislocation with an arbitrary Burgers vector as shown in Figure 1 is given as [1,3]

$$\sigma_{ij} = \frac{1}{d}\Sigma_{ij}\left(\hat{b},\hat{t}\right), \tag{1}$$

where d is the shortest distance from the field point to the dislocation line, $\hat{b}$ is the Burgers vector, $\hat{t}$ is the line sense vector and Σ_{ij} are the components of the angular stress factor matrix for an infinite dislocation. Now consider a finite segment as shown in Figure 2, the stress field about the segment using the so called integral formalism [1-6,9,10] is given by,

$$\sigma_{ij} = \frac{1}{2d}\left[-\cos(\gamma-\alpha)\Sigma_{mn} - \sin(\gamma-\alpha)\Sigma'_{mn}\right]_{\gamma_1}^{\gamma_2} \tag{2}$$

where

$$\Sigma_{mn} = \frac{1}{2}C_{mnip}b_s\left\{-\frac{\partial t_p}{\partial\gamma} + N_p(NN)^{-1}_{ik}\left[4\pi B_{ks} + \left(N\frac{\partial t}{\partial\gamma}\right)_{kr}S_{rs}\right]\right\} \tag{3}$$

and the derivative term is given by

$$\Sigma'_{mn} = \frac{1}{2}C_{mnip}b_s\left\{t_pS_{is} - \frac{\partial t_p}{\partial\gamma}\frac{\partial S_{is}}{\partial\gamma} + N_p(NN)^{-1}_{ik}\left[4\pi\frac{\partial B_{ks}}{\partial\gamma} + \left(N\frac{\partial t}{\partial\gamma}\right)_{kr}\frac{\partial S_{rs}}{\partial\gamma} - (Nt)_{kr}S_{rs}\right]\right\} \tag{4}$$

with C_{mnip} being the elastic constants, $\hat{t}$ and $\hat{b}$ the line sense vector and the Burgers vector, respectively. $\hat{p}$ is the vector from dislocation end point to the field point. $\hat{N} = \hat{t} \times \hat{p}$ is the vector normal defined by the field point and the dislocation segment. To discuss the terms in Equations (2) and (3), we define a local coordinate system as shown in Figure 2(a)-(b). In the figure, $\hat{t}$ is the unit vector along the dislocation line, and $\hat{m}$ and $\hat{n}$ are the unit vectors orthogonal to each other, which lie in the plane perpendicular to the dislocation line and they are given by

$$\hat{m} = \frac{\partial \hat{t}}{\partial \gamma}\cos\omega + \hat{N}\sin\omega \quad \text{and} \quad \hat{n} = -\frac{\partial \hat{t}}{\partial \gamma}\sin\omega + \hat{N}\cos\omega \tag{5}$$

Also,

$$B_{ks} = \frac{1}{4\pi^2}\int_0^{\pi}\left\{(mm)_{ks} - (mn)_{kr}(nn)^{-1}_{rj}(nm)_{js}\right\}d\omega \tag{6}$$

$$S_{ks} = -\frac{1}{\pi}\int_0^{\pi}(nn)^{-1}_{kj}(nm)_{js}\,d\omega \tag{7}$$

$$\frac{\partial S_{ks}}{\partial \gamma} = -\frac{1}{2\pi}\int_0^{2\pi}\left\{-F_{kj}(nm)_{js}\sin\omega + (nn)^{-1}_{kj}\left[(tm)_{js}\sin\omega - (nt)_{js}\cos\omega\right]\right\}d\omega \tag{8}$$

$$\frac{\partial B_{ij}}{\partial \gamma} = \frac{1}{8\pi^2}\int_0^{2\pi}\left\{\begin{array}{l} -\left[(mt)_{ij} + (tm)_{ij}\right]\cos\omega + (mn)_{ir}F_{rk}(nm)_{kj}\sin\omega \\ +\left[(tn)_{ir}\cos\omega - (mt)_{ir}\sin\omega\right](nn)^{-1}_{rk}(nm)_{kj} \\ -(mn)_{ir}(nn)^{-1}_{rk}\left[(tm)_{kj}\sin\omega - (nt)_{kj}\cos\omega\right] \end{array}\right\}d\omega \tag{9}$$

and

$$F_{rk} = (nn)^{-1}_{rs}\left\{(nt)_{sp} + (tn)_{sp}\right\}(nn)^{-1}_{pk} \tag{10}$$

The term $(nn)_{jk}$ is the Cristoffel stiffness matrix tensor and is given by

$$(nm)_{jk} = n_i C_{ijkp} m_p \tag{11}$$

and its inverse

$$(nn)^{-1}_{ij} = \frac{\varepsilon_{ism}\varepsilon_{jrw}(nn)_{sr}(nn)_{mw}}{2\varepsilon_{pgn}(nn)_{1p}(nn)_{2g}(nn)_{3n}} = (nn)^{-1}_{ji} \tag{12}$$

with ε_{ijk} being the permutation tensor.

The physical representation of the stress field of a finite segment is given in terms of rational segment representations by Eshelby and Laub [8], giving an analogy of current density flux connecting a wire immersed in a conducting liquid. Bacon et al. [9,10] reviewed the issue in terms of semi-infinite "hair-pin" arm dislocations which connect two end points of a segment. As shown by Asaro and Barnett [3] and Bacon *et al.* [9,10] when the field point is co-planar with an infinite dislocation or with a closed-loop dislocation configuration, the angular derivative term in Equation (2) drops, reducing to a simpler expression,

$$\sigma_{ij} = \frac{1}{2d}\left[-\cos(\gamma-\alpha)\Sigma_{mn}\right]_{\gamma_1}^{\gamma_2} \tag{13}$$

For a general three-dimensional problem, however, Equation (2) must be used.

3. Result and Discussion

In this section, we examine several dislocation configurations and perform numerical analysis to verify that the methodology presented in the previous section produces the correct stress fields. The main interest here is to numerically implement Equations (1) and (2). Consider a dislocation segment shown in Figure 2(a). To evaluate the stress field of a finite dislocation, two fundamental parameters are required. The first

being the dislocation line sense vector $\hat{t}$ and the second, normal vector $\hat{N}$ defined by the two end point of the segment and field point as shown in Figures 2-4.

Since no explicit expression for the stress field of a finite segment in an anisotropic medium is available, we first consider the isotropic case and use the isotropic elastic constants in equations (2)-(4) and compare the results with known closed form solutions. Next, comparison between isotropic and anisotropic cases is discussed. For numerical integration of Equations (6)-(9), a matrix version of Rhomberg integration was developed. The calculations are performed for the case of Mo single crystal for two cases, isotropic elasticity with the elastic properties:

$$\mu = 130\,\text{GPa},\ \nu = 0.309 \quad C_{11} = \mu\left(1 + \frac{1}{1-2\nu}\right),\ C_{12} = \mu\left(\frac{2\nu}{1-2\nu}\right) \text{ and } C_{44} = \mu$$

And anisotropic elasticity with

$$C_{11} = 460, C_{12} = 176 \text{ and } C_{44} = 110\,\text{GPa}.$$

Numerical Example

We consider a closed dislocation loop resembling a hexagon as shown in Figure 5. To avoid symmetry when evaluating the stress field and to generalize the argument, we stretch the hexagon vertices in an alternating manner along the vertical direction as shown in the figure. The resultant stress field just above the hexagon is evaluated on 100 x 100 square grid points (spaced by 4 Burgers vectors) using the integral formalism described in the previous sections. The recently developed dislocation dynamics code (*micro3d*) [11-13], which is based on isotropic elasticity is used to calculate the stress fields and the results are compared to the current method.

The stress field along the lateral direction is given in Figure 6. The percent difference between the isotropic solutions using the integral formalism, equations (2)-4), and the closed form solution using *mirco3d,* is given in Figure 7, showing that the maximum error is less than 0.015 %. Also in the figure we show the stress field for the case of anisotropic elasticity using the elastic constants given above. When compared to the isotropic case, the difference can be as high as 15%, especially close to the loop. However, the relative difference in the stress magnitude between the two cases decreases far away from the loop. This suggests that the use of isotropic elasticity for local dislocation-dislocation interaction (e.g. junction formation) may involve significant errors, but not for long-range interaction.

The calculations were performed on a 500 MHz DEC Alpha system. CPU time is measured for three different cases (Dislocation Dynamics, the integral formalism with isotropic elastic constants, and the third with full anisotropic elastic constants) and given in Table 1. In the table, it is noticeable that the CPU time for the case with anisotropic elasticity is as close to approximately 500 times higher than just using the dislocation dynamics code. Most of the time is spent on evaluation of the integrals in Equations (6)-(9). Therefore, it appears that direct calculations for dislocation dynamics in highly anisotropic media become computationally massive.

One way to resolve this computational problem as in for many other numerical simulations is to tabulate the closed integrals involved in the analysis, which requires the use of more memory. As shown in Figure 4, since only $\hat{N}$ and $\hat{p}$ vectors are required

to evaluate the integrals, one can specify these vectors in spherical coordinates, i.e. express $\hat{N}$ and $\hat{p}$ by three angles as shown in Figure 8, which are given as

$$\hat{p} = \begin{pmatrix} \sin\theta\cos\phi \\ \sin\theta\sin\phi \\ \cos\theta \end{pmatrix}, \tag{14}$$

$$\hat{N} = \cos(\lambda)\cdot\hat{e}_\theta + \sin(\lambda)\cdot\hat{e}_\varphi = \begin{pmatrix} \cos\phi\cos\lambda\cos\theta - \sin\phi\sin\lambda \\ \sin\phi\cos\lambda\cos\theta + \cos\phi\sin\lambda \\ -\cos\lambda\sin\theta \end{pmatrix}. \tag{15}$$

In the figure, the geometry is defined by only two distinct vectors, the line sense vector $\hat{t}$ and field vector $\hat{p}$, and $\hat{N} = \hat{t}$ x $\hat{p}$. Therefore, the fundamental parameters are only $\hat{N}$ and $\hat{p}$. In the actual dislocation dynamics, the values of the three angles are determined by the two vectors. To minimize the cost of evaluating $\sum_{ij}$ and $\sum'_{ij}$, linear interpolation method weighted by the volume of the eight rectangles around the interpolation point is used. Higher order interpolation methods could give better resolution but this aspect is under investigation.

Using 1 degree look up table as a function of three angles, θ, ϕ, λ and six components of $\sum_{ij}$ and $\sum'_{ij}$, we evaluated the stress field of the distorted hexagon in Mo. The Burgers vector in Equations (3) and (4) can add another degree of freedom. To avoid this complexity, we decompose the Burgers vector into three components and superimpose the stress field for each component to obtain the resultant field. Therefore, instead of having two look-up tables for $\sum_{ij}$ and $\sum'_{ij}$, there should be total of six tables. The errors of all the stress components between the direct integral method and the use of the look-up tables are given in Figure 8(a), yielding an average error of approximately

0.19 %. The memory required for the size of the look up table now becomes of concern since size of the estimated table is close to 3 Gb. This estimate comes from the following analysis. For 1 degree increment,

$$\text{Total number of points} = n_\theta n_\phi n_\lambda n_f n_b \tag{16}$$

where $n_\theta = 180$ is the number of grid points for θ, and $n_\phi = 360$ and $n_\lambda = 360$ are the grid points for ϕ and λ, respectively. $n_f = 12$ is the total number of stress components to interpolate for $\sum_{ij}$ and $\sum'_{ij}$ and $n_b = 3$ is the three components of the Burgers vector. Therefore, if we use single precision in the table, which is 4 bytes per number in memory, the total memory required becomes approximately 3.4 Gb. If we reduce the incremental angle by one half, the size becomes 8 times smaller and the error should increase by 8 times also. The plot of error using a 2-degree increment look-up table is given in Figure 8(b), yielding an average error of 0.75 percent. The size required for this case is approximately 500 Mb. One way to improve the method is by employing the approach by Bacon *et al.* [9,10] where they approximated a two-dimensional functional data by fitting and expressed as a Fourier expansion. In their analysis, they showed that only 5 terms in the series are required to give accuracy within 0.5 %. This method along with higher order interpolations that would require coarse mesh is currently under investigation and will be presented in the forthcoming articles.

Line Tension

Since the net force on a dislocation segment should include line tension force from the adjacent segments as well as the remote stress fields arising from other

dislocations, line tension in discrete dislocation dynamics models should be included to avoid any artifacts on dislocation patterning. For isotropic media, the treatment is well established using a tabular form [14], or explicit evaluation of a continuous dislocation bend with the same or different Burgers vectors [13]. For an anisotropic medium, we use the approach by Lothe [15]. The force on a dislocation bend in anisotropic media is given by

$$dF = \frac{1}{\lambda}\left(\frac{E(0)}{\sin\theta} - \frac{E(\theta)}{\tan\theta} + \frac{\partial E(\theta)}{\partial\theta}\right)dl \tag{17}$$

where λ is the distance from the bend and θ is the angle between the two dislocation segments around the bend. For a straight dislocation, the energy factor and its derivative terms, $E(\theta)$ and $\partial E(\theta)/\partial\theta$ in equation (17), are given by half of the stress factor and its derivative in equation (2), respectively [16].

4. Conclusion

A numerical methodology in terms of combination of speed and memory for the elastic interaction calculation of dislocations in anisotropic media has been discussed. To validate the methodology, comparisons of direct calculations using the isotropic elastic constants with a dislocation dynamics model are performed to show that the deviations from the exact solutions are within desired accuracy. Also, the comparison between isotropic and anisotropic elasticity shows that the error of the nearby stress field around a hexagon can be as high as 15 %, suggesting it is important to use anisotropic elasticity for short-range dislocation-dislocation interactions. We introduced a look-up table scheme to minimize heavy computational efforts for the integral evaluations within

a reasonable degree of accuracy. Linear Interpolation was used to avoid additional computational cost and memory. Higher order interpolation methods are currently under investigation. The result shows that the difference between the isotropic and anisotropic solutions around the hexagon becomes noticeably small with increasing distance. This suggests that one can use the explicit integral evaluation for near dislocation-dislocation interactions and isotropic elasticity for long-range interaction. Finally, although one must explicitly use the integral formalism to numerically calculate the different tables for the stress factor and its derivative terms, this has to be done only once for any given material and set of elastic constants, the results being stored for subsequent analysis.

Acknowledgment

This work was performed under the auspices of the U.S. Department of Energy by the University of California, Lawrence Livermore National Laboratory under Contract No. W-7405-Eng-48.

References

[1] L.M. Brown (1967), Phil. Mag., **15**, 363.

[2] V.L. Indenbom and S.S. Orlov (1968), Sov. Phys. Crystallography, **12**, No. 6, 849.

[3] R.J.Asaro and D.M.Barnett (1976), "Computer Simulation for Materials Applications, **20**. Part 2. Nuclear Metallurgy, ed. by R.J. Arsenault, J.R. Beeler, Jr., and J.A. Simmons, P313.

[4] R.J. Asaro and J.P. Hirth (1973), J. Phys. F: Metal Phys., **3**, 1659.

[5] J. Stolken (1998), Unpublished work.

[6] D. Raabe (1996), Z. Metallkd., **8**, No. 6, 493.

[7] V.B.Shenoey, R.V. Kukta and R. Philips (1999), submitted for publication.

[8] J.D. Eshelby and T. Laub (1967), Canadian J. of Physics, **45**, 887.

[9] D.J. Bacon, D.M.Barnett and R.O.Scattergood (1979), "Progress in Materials Science", 23, pp.51-263, ed. By B. Chalmers, J.W. Christian and T.B.Massalski, Pergamon Press Ltd.

[10] D.J. Bacon, D.M. Barnett and R.O. Scattergood (1979), Phil. Mag. A, **39**, No.2, 231.

[11] J.P. Hirth and M. Rhee and H.M. Zbib (1996), J. Computer-Aided Materials Design, **3**, 164.

[12] H.M. Zbib, M. Rhee, J.P. Hirth (1998), Int. J. Mech. Science, **40**, 113.

[13] M. Rhee, H.M. Zbib, J.P. Hirth, H. Huang and T. Diaz de la Rubia (1998), Modeling & Simulations in Mater. Sci. & Engr, **6**, 467

[14] B. Denvincre and M. Condat (1992), Acta Metall., **40**, No 10, 2629.

[15] J. Lothe (1967), Phil. Mag., **15**, 353.

[16] H. Schmid and H.O.K. Kirchner (1988), Phil. Mag. A, **58**, No. 6, 905.

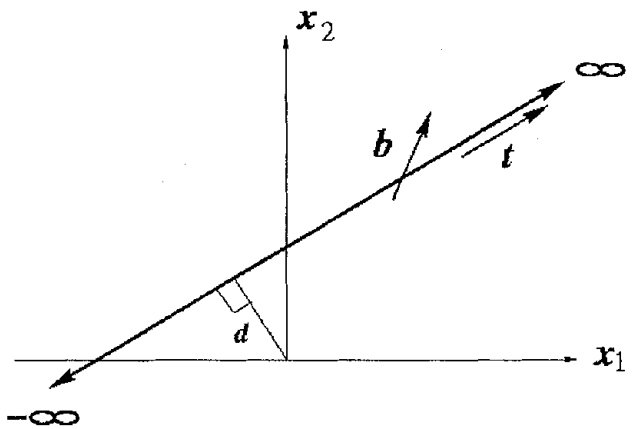

Figure 1 Coordinate system for the stress field of an infinite dislocation.

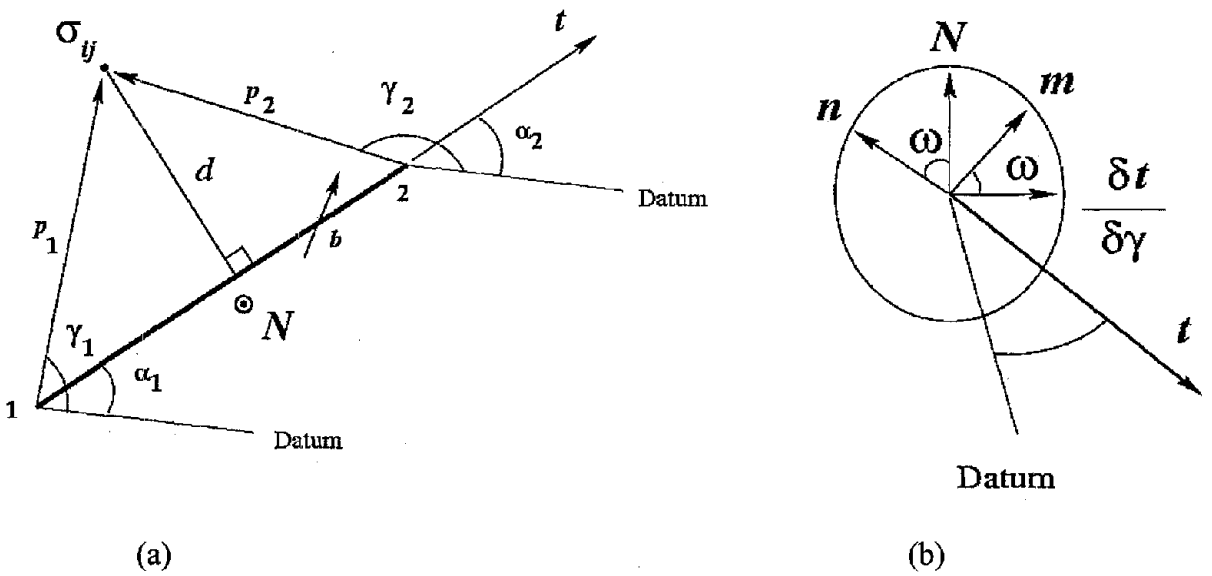

Figure 2 Coordinate system used to calculate stress field about a finite segment.

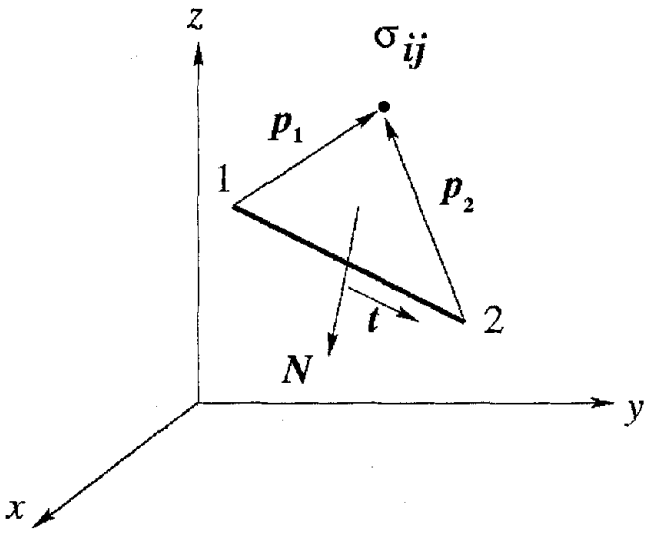

Figure 3 Illustration of evaluation of stress field in 3D space

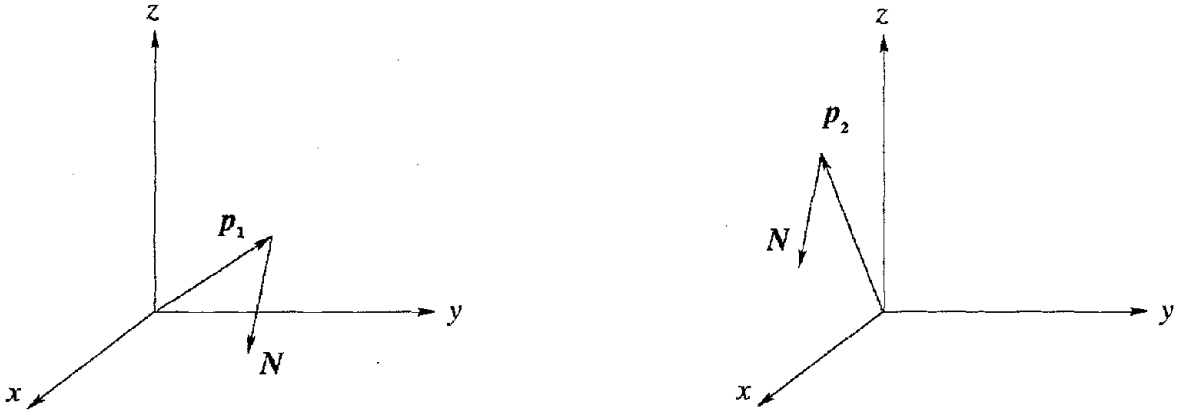

Figure 4 Schematic details of vectors required for the evaluation of configuration given in Figure 3.

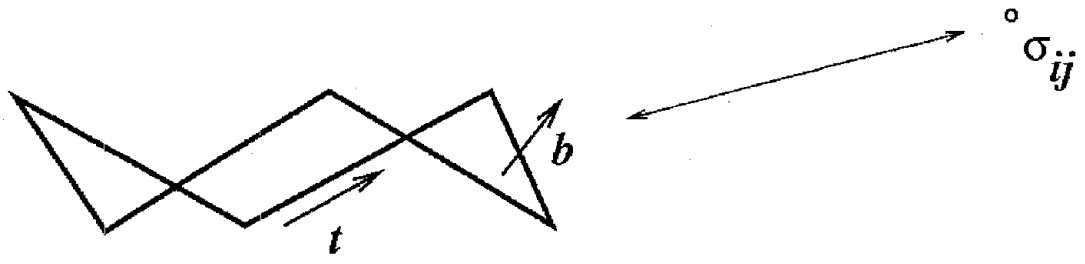

Figure 5 Geometry of a distorted hexagon to calculate the stress fields on a 100 x 100 grid points. The hexagon is stretched in the vertical direction to produce non-symmetry when evaluating the angular stress factor and derivative.

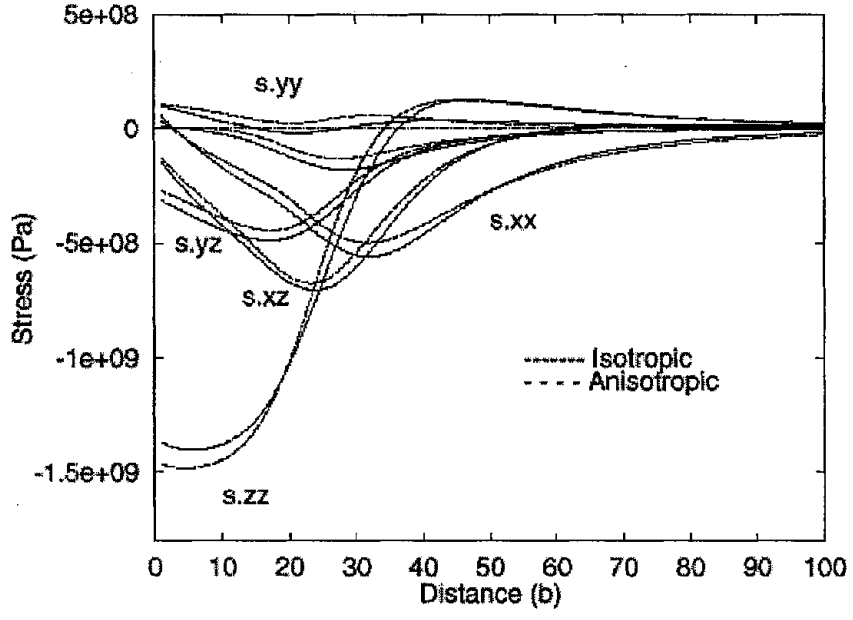

Figure 6 Stress distribution along horizontal direction about the distorted hexagon using both isotropic and anisotropic elasticity.

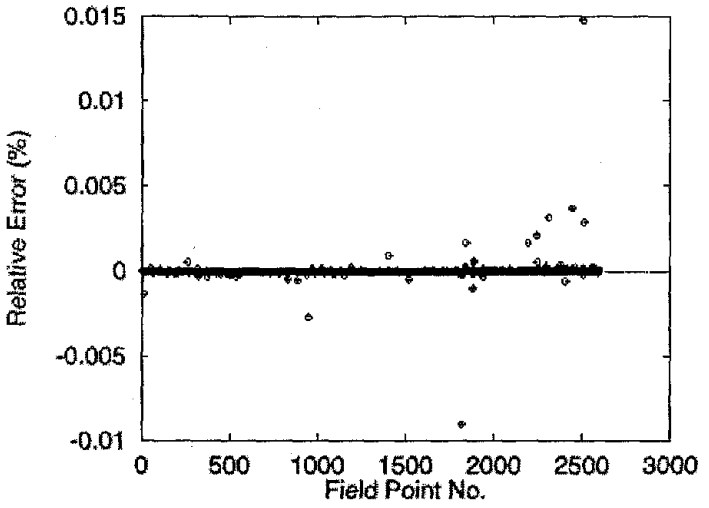

Figure 7 Relative error between the resultant stresses produced by the integral formalism with isotropic elastic constants and those by a dislocation dynamics code.

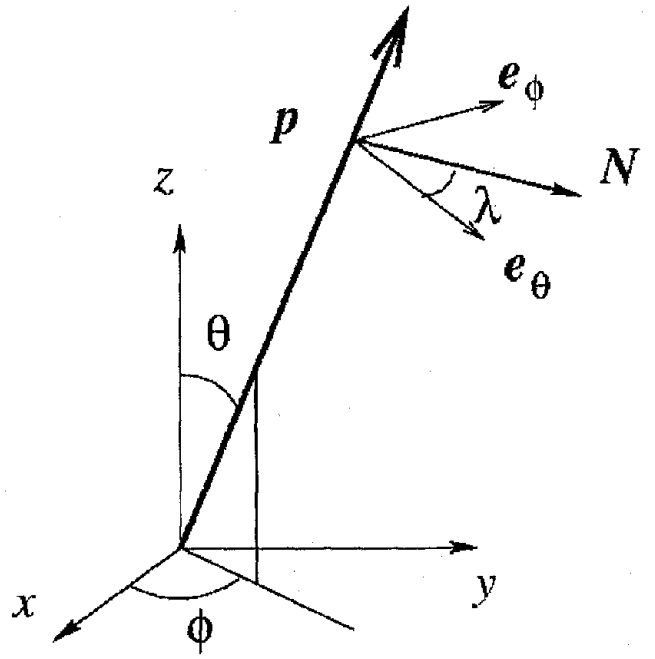

Figure 8 Parameterization of vector $\hat{p}$ and $\hat{N}$ using spherical coordinates.

(a)

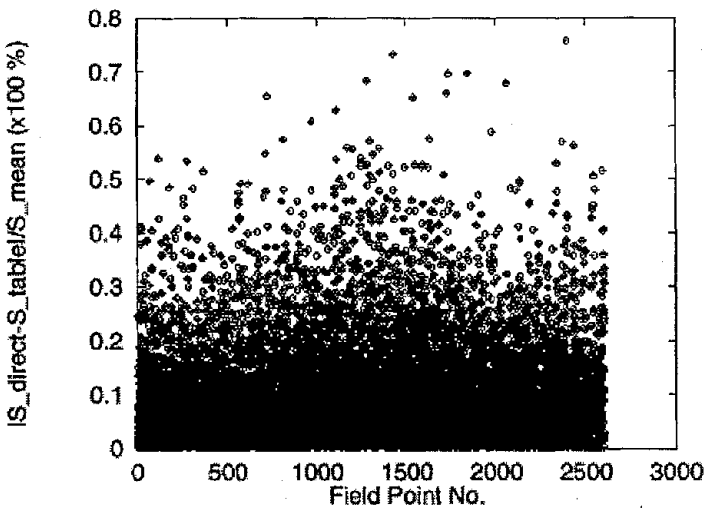

(b)

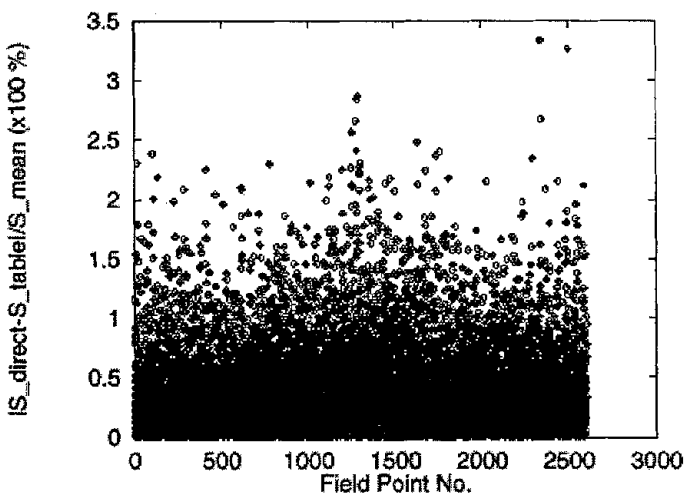

Figure 9 Absolute error (divided by the mean stress value) between the methods by direct evaluation of integrals and look-up tables with (a) 1 degree (b) 2 degree increment.

Table 1 CPU Time Comparisons

Method	CPU Time (sec.) (Dec Alpha 500 MHz)
Dislocation Dynamics Code (micro3d, WSU)	0.662
Integral Formalism Method	
Isotropic Contants	349.6
Anisotropic Constants	2540.9